Journal of Hepatocellular Carcinoma

Dovepress
Taylor & Francis Group

Open Access Full Text Article

ORIGINAL RESEARCH

NRF1-Induced lncRNA DDX11-AS1 Contributes to the Progression of Hepatocellular Carcinoma via Activating CA9 Expression and the MEK/ERK Pathway

Yingnan Li[1,2], Mengjiao Shi[1,3], Beibei Bie[4], Hongwei Tian[1,3], Jun Li[1,3], Zongfang Li[1–3], Jin Sun[1,3]

[1]Department of General Surgery, National-Local Joint Engineering Research Center of Biodiagnostics and Biotherapy, The Second Affiliated Hospital of Xi'an Jiaotong University, Xi'an, 710004, People's Republic of China; [2]Center for Tumor and Immunology, The Precision Medical Institute, The Second Affiliated Hospital of Xi'an Jiaotong University, Xi'an, 710115, People's Republic of China; [3]Shaanxi Provincial Clinical Research Center for Hepatic & Splenic Diseases, The Second Affiliated Hospital of Xi'an Jiaotong University, Xi'an, 710004, People's Republic of China; [4]Department of Pharmacy, Medical School, Xi'an Peihua University, Xi'an, 710125, People's Republic of China

Correspondence: Zongfang Li, Department of General Surgery, National & Local Joint Engineering Research Center of Biodiagnostics and Biotherapy, The Second Affiliated Hospital, Xi'an Jiaotong University, No. 157 West 5th Road, Xi'an, 710004, People's Republic of China, Email lzf2568@xjtu.edu.cn; Jin Sun, Department of General Surgery, National & Local Joint Engineering Research Center of Biodiagnostics and Biotherapy, The Second Affiliated Hospital, Xi'an Jiaotong University, No. 157 West 5th Road, Xi'an, 710004, People's Republic of China, Email jinsun2014@foxmail.com

Purpose: DDX11 antisense RNA 1 (DDX11-AS1) has been recognized for its strong correlation with hepatocellular carcinoma (HCC). Nevertheless, the exact biological functions and fundamental molecular processes of DDX11-AS1 in HCC require further in-depth investigation.

Methods: A comprehensive bioinformatics analysis was carried out to explore the expression of DDX11-AS1 and its clinical implication in HCC utilizing the TCGA data. qRT-PCR was employed to validate the expression of DDX11-AS1 in HCC tissues/cell lines. RNA fluorescence in situ hybridization (RNA-FISH) was used to observe the subcellular localization of DDX11-AS1 in HCC cells. Loss-of-function experiments, both in vitro and in vivo, were executed to elucidate the biological functions of DDX11-AS1 in HCC. RNA sequencing (RNA-seq) was employed to identify genes and signaling pathways potentially regulated by DDX11-AS1. Rescue experiments were conducted to validate that carbonic anhydrase IX (CA9) mediates DDX11-AS1 promoting HCC progression. The influence of nuclear respiratory factor 1 (NRF1) on the transcription of DDX11-AS1 was investigated through dual-luciferase reporter assays and ChIP-qPCR.

Results: The increased expression of DDX11-AS1 is positively associated with several aggressive clinical characteristics (pathologic T stage, histologic grade, AFP level, and vascular invasion), and is closely linked to unfavorable outcomes in HCC patients, acting as a separate hazardous factor for overall survival. DDX11-AS1 is predominantly situated in the nucleus of HCC cells. DDX11-AS1 knockdown impeded the growth, migration, and invasion capabilities of HCC cells in vitro, and reduced the tumor enlargement in a subcutaneous mouse model. RNA-Seq unveiled that silencing DDX11-AS1 lessened the expression of CA9 and suppressed the activity of the MEK/ERK signaling cascade in HCC cells. Rescue experiments uncovered that CA9 acts as a downstream target facilitating the cancer-causing roles of DDX11-AS1 in HCC. Furthermore, DDX11-AS1 was revealed to be transcriptionally regulated by NRF1.

Conclusion: DDX11-AS1, a NRF1-induced lncRNA, facilitates HCC development by upregulating CA9 expression and activating the MEK/ERK signaling cascade.

Keywords: hepatocellular carcinoma, DDX11-AS1, CA9, MEK/ERK signaling, NRF1

Introduction

Hepatocellular carcinoma (HCC) represents the most prevalent form of primary liver cancer, holding the sixth position in tumor prevalence and being the third leading global cause of cancer-associated mortality.[1] The etiology of HCC is

Received: 9 January 2025
Accepted: 29 April 2025
Published: 7 May 2025

© 2025 Li et al. This work is published and licensed by Dove Medical Press Limited. The full terms of this license are available at https://www.dovepress.com/terms.php and incorporate the Creative Commons Attribution – Non Commercial (unported, v4.0) License (http://creativecommons.org/licenses/by-nc/4.0/). By accessing the work you hereby accept the Terms. Non-commercial uses of the work are permitted without any further permission from Dove Medical Press Limited, provided the work is properly attributed. For permission for commercial use of this work, please see paragraphs 4.2 and 5 of our Terms (https://www.dovepress.com/terms.php).

multifaceted, encompassing viral infections like hepatitis B and C (HBV and HCV), deleterious lifestyle choices like excessive alcohol consumption and smoking, exposure to environmental toxins like aflatoxin, non-alcoholic fatty liver disease (NAFLD), and genetic mutations and the activation of critical signaling pathways.[2] Despite recent advancements in diagnostic techniques and therapeutic approaches for HCC, notably through the implementation of targeted therapies and immunotherapeutic agents, therapeutic outcomes remain suboptimal. This is largely attributable to the asymptomatic nature of HCC in its early stages, challenges in early detection, and the fact that a significant proportion of patients are already in the late stage when diagnosed, thereby restricting therapy options and leading to unsatisfactory clinical outcomes.[3] Consequently, developing potent biomarkers and therapeutic targets is vital for enhancing the diagnosis and treatment of HCC.

Long noncoding RNAs (lncRNAs) are a category of RNA molecules distinguished by their lengths surpassing 200 nucleotides and their inability to code for proteins, possessing dynamic regulatory roles.[4] Numerous studies over the past decade indicate that lncRNAs exert pivotal functions in the advancement of different cancers by controlling gene expression across multiple layers, involving transcriptional, post-transcriptional, and epigenetic regulation.[5] For HCC, numerous lncRNAs have been disclosed to be misregulated, contributing to HCC development as oncogenes or tumor suppressors by influencing cell proliferation, apoptosis, migration, invasion, and angiogenesis.[6]

DDX11 antisense RNA 1 (DDX11-AS1), also referred to cohesion regulator noncoding RNA (CONCR), is a non-coding transcript diverging from the DDX11 gene on human chromosome 12p11.21.[7] DDX11-AS1 was first discovered as a cell cycle-regulated lncRNA, which can affect cell cycle process and DNA duplication through modulating sister chromatid cohesion. Recent studies have unveiled that DDX11-AS1 is upregulated across multiple cancer types and contributes to tumor progression by participating in various cancer-associated biological activities, including cell proliferation, migration, invasion, and resistance to drugs. In breast cancer (BC), the elevated DDX11-AS1 expression is linked to higher pathological grades and lymph node metastasis, facilitating cell growth, migration, and invasion through the miR-30c-5p/MTDH pathway, and increasing adriamycin (ADR) resistance through LIN28A-mediated stabilization of ATG12 mRNA.[8,9] Regarding esophageal cancer (EC), DDX11-AS1 exhibits the ability to accelerate EC cell propagation and migration via the miR-514b-3p/RBX1 pathway, and increases paclitaxel resistance through activating the TAF1/TOP2A signaling axis.[10,11] As for HCC, recent studies indicate that DDX11-AS1 significantly contributes to HCC progression by enhancing cell proliferation via the PARP1/p53 and miR-34a-3p/TRAF5 axis and inhibiting sorafenib-induced ferroptosis through the Nrf2-Keap1 pathway.[12–14] However, the exact biological functions and underlying molecular mechanism of DDX11-AS1 in HCC need further in-depth investigation.

Carbonic anhydrase IX (CA9) is a transmembrane zinc metalloenzyme that regulate intracellular pH (pHi) and extracellular pH (pHe), and has been proven to be widely implicated in cancer progression via its catalytic activity and/or non-catalytic functions.[15] For HCC, the elevation of CA9 was revealed to be linked to the unfavorable prognoses, and can facilitate the HCC progression by influencing cell growth, apoptosis as well as epithelial-mesenchymal transition (EMT).[16–18] Currently, it is unclear whether there is a regulatory relationship between CA9 and DDX11-AS1 in HCC.

The MEK/ERK pathway is the most classical and well-studied crucial signaling cascade among all MAPK signal transduction pathways, and plays a pivotal role in tumor occurrence and development.[19] In HCC, the MEK/ERK signaling pathway is activated in more than 50% of human HCC cases.[20] It has been discovered that many lncRNAs can promote the progression of HCC via activating the MEK/ERK signaling pathways, such as HOXD-AS1 and HOXD-AS2.[21,22] However, the effect of DDX11-AS1 on the MEK/ERK signaling in HCC is still unclear.

This research conducted a comprehensive investigation into the expression patterns of DDX11-AS1 and its possible clinical importance, biological roles, and molecular mechanisms in HCC. The findings deepen our understanding of how DDX11-AS1 contributes to HCC development, indicating its potential as a diagnostic biomarker and therapeutic target for HCC.

Materials and Methods

Bioinformatics Investigation Employing the TCGA Data

RNA-seq data and associated clinicopathological details were retrieved from The Cancer Genome Atlas (TCGA) (https://portal.gdc.cancer.gov/) for a cohort consisting of 374 hCC patients and 50 non-tumorous tissue samples. The values of

TPM (transcripts per million reads) were acquired through transforming and normalizing the HTSeq-FPKM data using a log2 conversion. All bioinformatics processing based on TCGA data was executed with R (version 4.2.1). The expression of DDX11-AS1 in HCC and its relevance with clinicopathological traits were assessed using the R package "ggplot2". The connection between the DDX11-AS1 expression and the prognosis of HCC patients was evaluated utilizing the R packages "Survival" and "Survminer". The Cox proportional hazards regression model was employed to screen the hazardous factors influencing overall survival (OS), while the nomogram forecast model and calibration plot were established utilizing the R packages "rms" and "survival" to estimate the 1-, 3-, and 5-year OS chances according to identified hazards factors. Utilizing the "pROC" R package, the receiver operating characteristic (ROC) curves were created to estimate diagnostic and prognostic performance. The lncATLAS online tool (https://lncatlas.crg.eu/) was used to forecast the subcellular localization of DDX11-AS1.[23]

Collection of Human HCC Samples

Eighteen HCC tissue samples and their corresponding benign liver tissues were sourced from the biobank of the National and Local Joint Engineering Research Center of Biodiagnostics and Biotherapy at the Second Affiliated Hospital of Xi'an Jiaotong University, Xi'an, China. All specimens were pathologically verified and had not undergone radiotherapy or chemotherapy before acquisition. Post-dissection, the specimens were promptly frozen using liquid nitrogen and preserved at −80°C. Informed consent was acquired from each patient, and the study was approved by the Ethics Committee of Xi'an Jiaotong University Health Science Center (No. 2020–738). All procedures were carefully handled to meet the guidelines of the Declaration of Helsinki.

Cell Culture

Human HCC cell lines (Bel-7402, Bel-7404, SMMC-7721, Hep3B, Huh7) along with the normal hepatocyte cell line L-O2 were acquired from the Cell Bank of Type Culture Collection of the Chinese Academy of Sciences located in Shanghai, China. All cell lines were cultured in Dulbecco's Modified Eagle's Medium (DMEM, Cytiva, USA) containing 10% fetal bovine serum (Corning, USA), 100 units/mL penicillin and 100 μg/mL streptomycin (Biosharp, China) in an incubator with 5% CO_2 at 37°C.

Vector Construction, LncRNA Smart Silencer and Small Interfering RNA (siRNA) Synthesis

Silencing of DDX11-AS1 was achieved using the LncRNA Smart Silencer purchased from RiboBio (Guangzhou, China), which includes three siRNAs and three antisense oligonucleotides (ASOs) targeting the following sequences: 5'-CUCAUUCCUCUGCCUACAA-3'; 5'-GGAGAAUGAAUUCAUGCUA-3'; 5'-CCUUAUCACUGUGGCAGAA-3'; 5'-UGUGACCAUCGUGGAAGCCC-3'; 5'-GCUGCUACUGUGGAGGACGU-3'; 5'-AAUGAGAGAGCCAAGGCCUU-3'. NRF1 knockdown was achieved using the siRNAs aimed at NRF1 (5'-GAUGAAGACUCGCCUUCUU-3') and a negative control siRNA (5'-UUCUCCGAACGUGUCACGU-3'), both obtained from RiboBio (Guangzhou, China). CA9 overexpression vector (EX-Z5727-Lv105-B) was purchased from GeneCopoeia, USA. The open reading frame (ORF) of human NRF1 was amplified and cloned into the pCDH-CMV-MCS-EF1-CopGFP-T2A-Puro mammalian expression plasmid (#72263; Addgene, USA) for NRF1 overexpression. The DDX11-AS1 promoter (the 2000 bp region upstream of the transcription start site) was amplified and inserted into the pGL3-Basic vector (Promega, USA) to obtain the luciferase reporter vector for detecting the activity of the DDX11-AS1 promoter. The jetPRIME® Versatile DNA/siRNA Transfection Reagent (Polyplus, France) was employed to perform transfection experiments. Supplementary Table S1 lists the primers utilized for vector construction.

Quantitative Real-Time PCR (qRT-PCR)

TRNzol Universal Reagent (Tiangen, China) and PARIS™ Kit (Thermo Fisher Scientific, USA) were used to extract total RNA and to separate the nuclear and cytoplasmic RNA, respectively. cDNA for qRT-PCR was synthesized using EasyScript® One-Step gDNA Removal and cDNA Synthesis SuperMix (Transgene, China), followed by qRT-PCR with

TransStart® Top Green qPCR SuperMix (Transgene, China). Samples underwent normalization against β-actin, and the relative expression values were examined employing the $2^{-\Delta\Delta Ct}$ method. All qRT-PCR primers employed in this research are detailed in Supplementary Table S1.

RNA Fluorescent in Situ Hybridization (RNA-FISH)

The RNA-FISH was performed using the Ribo™ Fluorescent in Situ Hybridization Kit (RiboBio, China) adhering to the guidelines provided by the manufacturer. In summary, the cells were grown on glass coverslips within a 24-well plate. Upon achieving 60% cell confluence, the cells were stabilized utilizing 4% paraformaldehyde and permeabilized with 0.5% Triton X-100. The cells subsequently underwent blocking with a prehybridization buffer maintained at 37°C for 30 minutes, followed by overnight incubation with 20 μM DDX11-AS1 FISH Probe Mix (Cy3) (RiboBio, China) at the same temperature. After rinsing with Hybridization Wash Buffer, cell nuclei underwent counterstaining with 4',6-Diamidino-2-Phenylindole (DAPI). Cells placed on glass coverslips were transferred to a glass slide for observation under a fluorescence microscope. U6 and 18S rRNA served as indicators for distinguishing nuclear and cytoplasmic positions, respectively. The FISH Probe Mixes aimed at U6 (lnc110101) and 18S (lnc110102) were purchased from RiboBio, Guangzhou, China.

Cell Viability Assay

In each well, a total of 5×10^3 cells were cultured in 96-well plates and exposed to CCK-8 reagent (Yeasen, China) for 90 minutes at 37 °C, and the optical density (OD) at 450 nm was detected employing a multifunctional microplate reader.

Clonogenic Survival Assay

Cells were planted onto 6-well plates, maintaining a concentration of 800 cells/well, incubated in a full medium over a period of 7 days. Upon the appearance of observable colonies, the cells were stabilized using 4% paraformaldehyde for 20 minutes. Colonies were imaged and counted following coloring with 0.1% crystal violet.

Cell Cycle and Apoptosis Assessment by Flow Cytometry

To analyze the cell cycle, cells underwent fixation in 70% chilled ethanol at 4 °C for overnight, followed by staining with a Cell Cycle Assay Kit (Dojindo, Japan). To analyze apoptosis, newly harvested cells underwent staining with the Annexin V-FITC/PI Apoptosis Detection Kit (Yeasen, China). FlowJo software (BD Biosciences, USA) was employed to measure the distribution of cells across different cell cycle phases and the percentage of apoptotic cells.

Cell Migration and Invasion Examinations by Transwell

The capacities of cells to migrate and invade were assessed through the use of both Matrigel-uncoated and coated 24-well transwell chambers, fitted with 8.0 μm transparent PET membranes (353097/354480, Corning, USA). In total, 5×10^4 cells were reconstituted in 200 μL of a serum-free solution and placed in the upper chamber. Culture medium, enriched with 10% fetal bovine serum (FBS), filled the lower chamber to act as a chemical attractant. After a 24-hour period for migration tests or 48 hours for invasion tests, the cells attached to the inside of the PET membrane were eliminated through wiping, and external cells were stabilized using 4% paraformaldehyde. Cells that had migrated and invaded were colored using crystal violet and examined employing a microscope (100×) to count.

Animal Experiments

Four-week-old female BALB/c nude mice were obtained and housed at the Laboratory Animal Center of Xi'an Jiaotong University. The mice were arbitrarily split into two groups, each consisting of five individuals. Subcutaneous injections of 0.1 mL DDX11-AS1-silenced or negative control Bel-7402 cells (2×10^6 cells) were administered into the right flank of each nude mouse. The size of the tumors was gauged on a weekly basis using a vernier caliper, and their volumes were determined by the formula: volume = (length × width^2)/2. Upon completing the experiment, the mice were euthanized, and their xenograft tumors were surgically removed and weighed. The animal experiments were carried out adhering to

the procedures established by the Animal Experimentation Ethics Committee of Xi'an Jiaotong University and the guidelines of the Declaration of Helsinki.

Western Blot

Total proteins isolated with WB Super RIPA Lysis Buffer (Haigene, Harbin, China) were resolved through SDS-PAGE using the Precast Protein Improve Gels (4–20%; Yeasen, China), followed by their transfer onto 0.22 μm PVDF membranes (Elabscience, USA). The transferred membranes were treated with Western Blot Rapid Blocking Buffer (Biosharp, China) for blocking and then incubated with primary antibodies overnight at 4°C. After reacting with an HRP-linked goat anti-rabbit IgG (H+L) secondary antibody (1:5000; AS028, ABclonal, China) at room temperature for one hour, the luminescence signal was detected using the Sensitive ECL Detection Kit (Proteintech, USA) and recorded with a chemiluminescence imager. β-Actin or GAPDH served as endogenous references. Supplementary Table S2 details the primary antibodies utilized for Western blotting in this study.

Immunohistochemistry (IHC) Staining

4-μm-thick sections were sliced from paraformaldehyde-fixed tissues, and used for IHC staining by employing an Immunohistochemical Kit (Abs957, Absin, China) adhering to the manufacturer's protocol. In brief, the dewaxed sections were incubated with the primary antibody for 20 minutes at 37°C after antigen retrieval and blocking, and then treated with an enzyme-labeled secondary antibody for 10 minutes. After diaminobenzidine (DAB) color development and hematoxylin redyeing, the sections were sealed and then photographed with a microscope. The primary antibodies used for IHC included Ki67 (1:100; PAC047Hu01, Cloud-Clone) and PCNA (1:2000; 10,205-2-AP, Proteintech).

RNA-Sequencing (RNA-Seq) and Associated Bioinformatics Study

The total RNA was isolated utilizing the TRNzol Universal Reagent (Tiangen, China) and sent to the Biomarker Biotechnology Corporation (Beijing, China) to perform RNA-seq. RNA integrity was examined by Agilent 2100 system (Agilent Technologies, USA). The NEBNext UltraTM RNA Library Prep Kit for Illumina (NEB, USA) was employed to create sequencing libraries, followed by sequencing on the Illumina HiSeq Xten platform (Illumina, USA). Using TopHat2, the paired-end reads underwent filtration and alignment with the human reference genome (GRCh38/hg38). The levels of transcript expression were measured by the ratio of fragments per kilobase of transcript to every million fragments mapped (FPKM). The EBSeq algorithm was employed to pinpoint differentially expressed genes (DEGs) (FDR < 0.05, $|\log2FC| \geq 0.6$). The DAVID online tool (https://david.ncifcrf.gov/) was adopted to perform the enrichment analysis of GO and KEGG pathways, and GO terms and KEGG pathways terms that were statistically significant were selected based on a *p*-value criterion below 0.05.

Dual-Luciferase Reporter Examination

Bel-7402 cells were co-transfected with reporter vectors (pGL3-DDX11-AS1), pRL-TK, NRF1-targeting siRNA (siNRF1), or the NRF1 expression vector (OE-NRF1) using jetPRIME® Versatile DNA/siRNA Transfection Reagent (Polyplus, France) for 36 hours. The luciferase activity was subsequently assessed using the Dual Luciferase Reporter Gene Assay Kit (Yeasen, China), while the relative promoter activity was ascertained by standardizing Firefly luciferase activity against Renilla luciferase activity.

Chromatin Immunoprecipitation (ChIP)

Bel-7402 cells were cultured in 15 cm dishes and transfected with either NRF1 overexpression (OE-NRF1) or empty vector (OE-NC). Forty-eight hours post-transfection, the cells underwent cross-linking with 1% formaldehyde, followed by a ChIP assay utilizing the SimpleChIP® Enzymatic Chromatin IP Kit (9003, CST). In brief, chromatin was fragmented using micrococcal nuclease, and 2% was retained as input. Using 5 μg of ChIP-grade NRF1 antibody (A3252, Abclonal) and Rabbit IgG Isotype Control (ab171870, Abcam), 10 μg of fragmented chromatin underwent immunoprecipitation. After inverting the cross-links, the DNA obtained through immunoprecipitation was purified and

used to perform the qRT-PCR with the ChIP-qPCR primers detailed in Supplementary Table S1. To calculate the input DNA percentage, the following formula was applied: Percent input = $2\% \times 2^{(\text{C[T] 2\% input sample} - \text{C[T] IP sample})}$.

Statistics

All statistical analyses were conducted employing GraphPad Prism version 10. The Student's *t*-test and one-way ANOVA methods were employed to evaluate the variances between two groups and across various groups, respectively. To evaluate DDX11-AS1 expression in HCC tissues, the Mann-Whitney *U* test was applied to unpaired samples, and the Wilcoxon signed-rank test was adopted for paired samples. Statistical significance was established by setting a *p*-value threshold below 0.05.

Results

Bioinformatics Investigation of DDX11-AS1 Expression and Its Clinical Relevance in HCC Based on TCGA Data

To elucidate the clinical importance of DDX11-AS1 in HCC, we thoroughly examined its expression and clinical relevance using TCGA data, which includes RNA-seq and clinicopathological information. DDX11-AS1 was found to be markedly elevated in both unpaired and paired HCC tissues as opposed to normal liver tissues (Figure 1A and B), and its upregulation correlated strongly with pathologic T stage, histologic grade, vascular invasion, and AFP level (Figure 1C–F). Survival analysis disclosed that higher DDX11-AS1 expression was significantly associated with poorer overall survival (OS), disease-specific survival (DSS) and progression-free interval (PFI) (Figure 1G–I). Univariate Cox regression analysis indicated significant associations between OS of HCC patients and DDX11-AS1 expression level (HR = 1.497, $p = 0.022$), T stage (HR = 2.598, $p < 0.001$), and M stage (HR = 4.077, $p = 0.017$) (Figure 1J). Multivariate Cox regression assessment further uncovered that the DDX11-AS1 level (HR = 1.719, $p = 0.017$) was a separate hazards factor influencing the OS of HCC patients (Figure 1K). The nomogram forecast model was developed using the prognostic risk factors of DDX11-AS1 expression, T stage, and M stage to estimate 1-, 3-, and 5-year OS potential in HCC patients (Figure 1L), which was highly accurate and stable during the calibration tests (Figure 1M). Additionally, ROC curves demonstrated that DDX11-AS1 expression could effectively predict HCC (AUC = 0.969) and 1-, 3-, and 5-year outcomes for OS (AUC = 0.709, 0.653, 0.652), DSS (AUC = 0.781, 0.680, 0.637), and PFI (AUC = 0.671, 0.584, 0.804) (Figure 1N–Q).

Experimental Validation of DDX11-AS1 Expression in HCC

To confirm the expression trends of DDX11-AS1 in HCC, we initially evaluated its expression in eighteen pairs of HCC tissues and corresponding nearby non-cancerous tissues that we gathered. The findings exhibited that DDX11-AS1 was markedly elevated in tumor specimens as opposed to nearby non-cancerous liver specimens (Figure 2A), corroborating our previous bioinformatics analysis. Subsequently, we examined the expression of DDX11-AS1 in five HCC cell lines (Bel-7402, Bel-7404, SMMC-7721, Hep3B, and Huh7) as well as in the human normal liver cell line L-O2, and the results unveiled that DDX11-AS1 was elevated across multiple HCC cell lines (Figure 2B).

Furthermore, to elucidate the subcellular distribution of DDX11-AS1 in HCC cells and to shed light on its functional and mechanistic studies, we initially investigated the subcellular positioning of DDX11-AS1 utilizing the LncATLAS online tool. As illustrated in Figure 2C and D, DDX11-AS1 demonstrated a predominantly nuclear distribution across multiple cell types, including the hepatoma cell line HepG2. Subsequently, the subcellular positioning of DDX11-AS1 in Bel-7402 cells was examined by RNA-FISH, revealing that DDX11-AS1 could be observed in both the nuclear and cytoplasmic areas of Bel-7402 cells (Figure 2E). To further validate this observation, we performed a fractionation experiment to separate cytoplasmic and nuclear RNA from Bel-7402 cells, followed by quantification of DDX11-AS1 transcript levels by qRT-PCR, and the results displayed a significantly higher concentration of DDX11-AS1 in the nuclear fraction compared to the cytoplasmic fraction (Figure 2F). To sum up, these findings suggest that DDX11-AS1 is localized in both the nuclear and cytoplasmic regions of HCC cells, with a higher abundance in the nucleus.

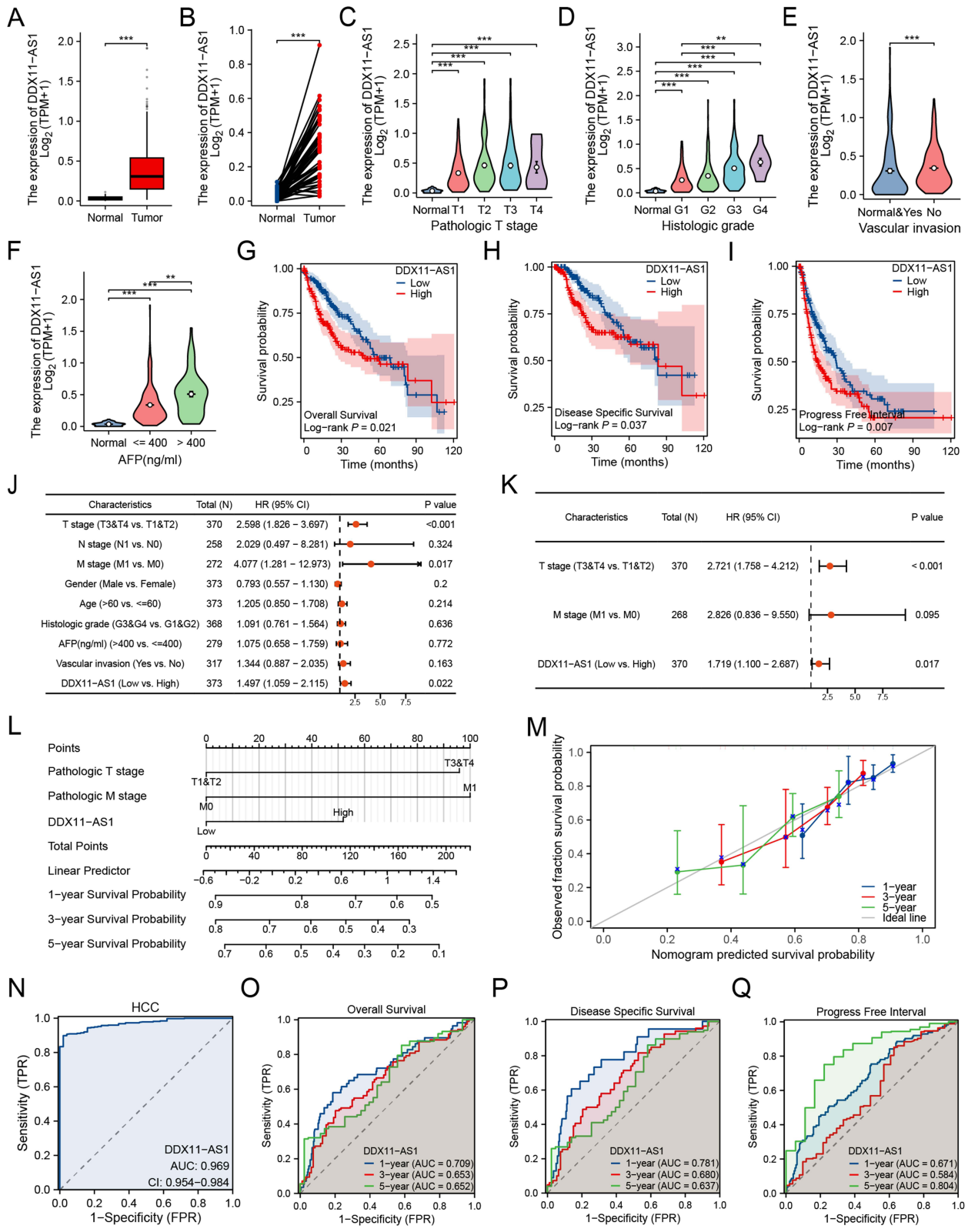

Figure 1 Bioinformatics analysis of DDX11-AS1 expression and its clinical significance in HCC. The DDX11-AS1 expression in unpaired (**A**) and paired (**B**) HCC tissues were analyzed using TCGA data. Correlation analysis of DDX11-AS1 expression with pathologic T stage (**C**), histological grade (**D**), vascular invasion (**E**) and AFP level (**F**). Relationship of the DDX11-AS1 expression with overall survival (**G**), disease-specific survival (**H**), and progression-free interval (**I**) was evaluated using TCGA data. Forest plot illustrating the results of univariate (**J**) and multivariate (**K**) Cox regression analysis of DDX11-AS1 expression for overall survival. (**L**) The nomogram predicting 1-, 3- and 5-year overall survival. (**M**) Calibration curves of the nomogram prediction model. Diagnostic or prognostic ROC curves of DDX11-AS1 for HCC (**N**), 1-, 3-, 5-year overall survival (**O**), 1-, 3-, 5-year disease-specific survival (**P**) and 1-, 3-, 5-year progress-free interval (**Q**). $^{**}p < 0.01$, $^{***}p < 0.001$.

https://doi.org/10.2147/JHC.S516656

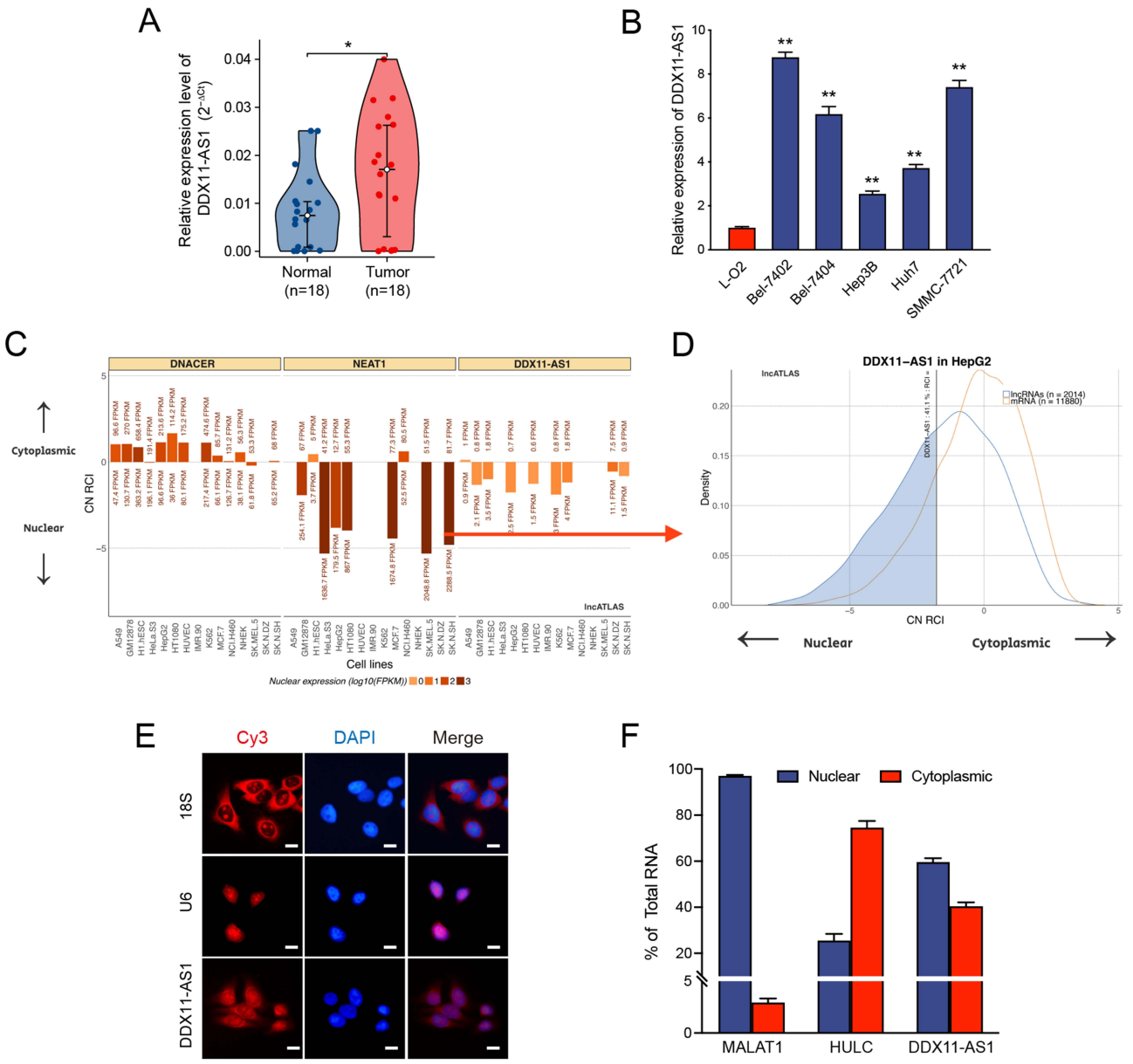

Figure 2 Experimental validation of the expression status of DDX11-AS1 in HCC. The expression status of DDX11-AS1 in 18 pairs of HCC tissues (**A**) and cell lines (**B**) were detected by qRT-PCR. (**C and D**) The subcellular localization of DDX11-AS1 in various cell types was predicted by lncATLAS. (**E**) The subcellular location of DDX11-AS1 in Bel-7402 cells was detected by RNA-FISH, with U6 and 18S serving as positive controls for nuclear and cytoplasmic localization, respectively (scale bar = 20 μm). (**F**) The abundance of DDX11-AS1 in the nuclear and cytoplasmic fractions of Bel-7402 cells was evaluated by qRT-PCR, with MALAT1 and HULC serving as positive indicators for nuclear and cytoplasmic lncRNA, respectively. *$p < 0.05$, **$p < 0.01$.

Downregulation of DDX11-AS1 Impairs the Capacities of Proliferation, Migration, and Invasion of HCC Cells in Vitro

To illustrate the biological functions of DDX11-AS1 in HCC in *vitro*, we conducted loss-of-function experiments using the Bel-7402 and SMMC-7721 cell lines, both of which exhibit elevated DDX11-AS1 expression. As illustrated in Figure 3A, the LncRNA Smart Silencer was capable of successfully silencing DDX11-AS1. Following this, the impact of DDX11-AS1 suppression on cell propagation was determined through CCK-8 and clonogenic survival assays, which exhibited a significant inhibition of HCC cell proliferation upon DDX11-AS1 muting (Figure 3B and C). Flow cytometric analysis was utilized to estimate the impact of DDX11-AS1 knockdown on cell cycle distribution and apoptosis rates after staining with PI and/or annexin V, and the results uncovered that silencing DDX11-AS1 markedly

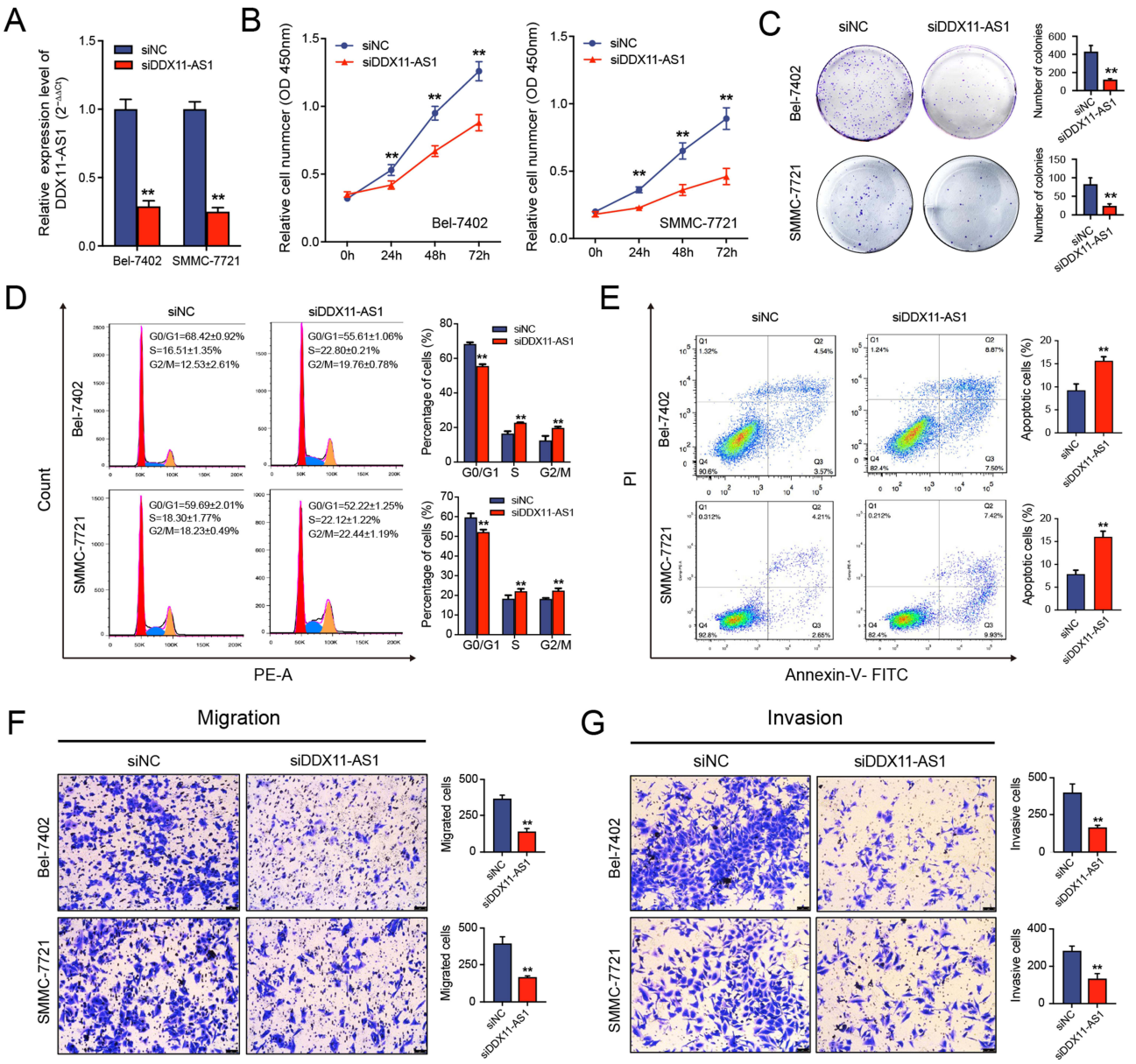

Figure 3 Downregulation of DDX11-AS1 represses the HCC progression in vitro. (**A**) The knockdown efficiency of DDX11-AS1 in Bel-7402 and SMMC-7721 cells was examined by qRT-PCR. The effect of DDX11-AS1 knockdown on the proliferation of HCC cells was evaluated by CCK-8 (**B**) and colony formation assays (**C**). The effect of DDX11-AS1 knockdown on cell cycle (**D**) and apoptosis (**E**) was detected by flow cytometry. The effect of DDX11-AS1 knockdown on the migration (**F**) and invasion (**G**) of HCC cells was assessed by transwell assay, scale bar =100 μm. siNC, negative control; siDDX11-AS1, DDX11-AS1 knockdown. $^{**}p < 0.01$.

caused the halt of cells at the S and G2/M phases of the cell cycle and promoted apoptosis (Figure 3D and E). Moreover, the transwell assay indicated that DDX11-AS1 knockdown notably impaired the migratory and invasive capabilities of HCC cells (Figure 3F and G). In summary, our findings unveiled that reducing DDX11-AS1 levels can diminish the cancerous biological characteristics in *vitro*.

The Suppression of DDX11-AS1 Leads to the Inhibition of HCC Cell Growth in the Subcutaneous Xenograft Nude Mouse Model

To evaluate the influence of DDX11-AS1 knockdown on HCC tumor growth in vivo, subcutaneous xenograft models were created using Bel-7402 cells in nude mice. As indicated in Figure 4A–C, DDX11-AS1 knockdown caused a marked reduction in both the volume and mass of xenograft tumors, in contrast to the negative control group. Additionally, IHC

https://doi.org/10.2147/JHC.S516656

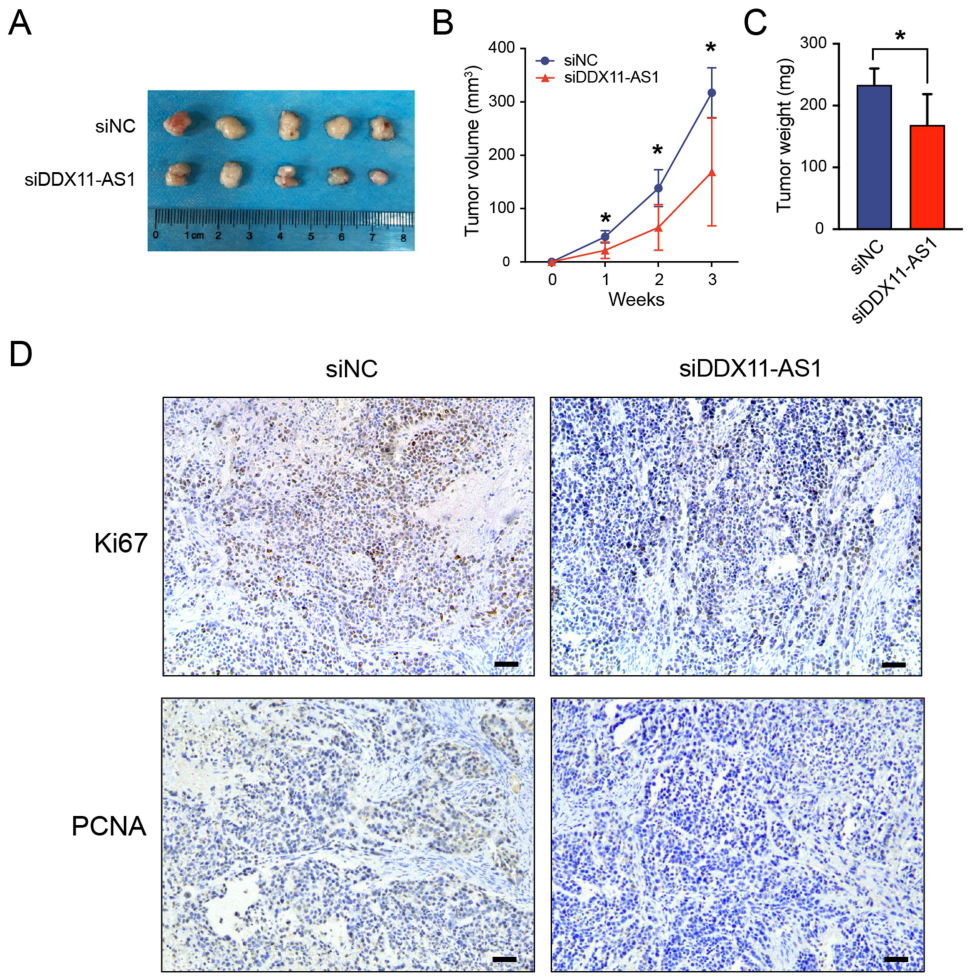

Figure 4 Knockdown of DDX11-AS1 inhibits HCC growth in a subcutaneous xenograft nude mouse model. (**A**) Photograph of dissected subcutaneous tumors at sacrificed time. (**B**) The volume of the subcutaneous tumors was measured every 7 days after implantation. (**C**) Tumor weight of dissected subcutaneous tumors at sacrificed time. (**D**) The expression of proliferative markers Ki67 and PCNA in subcutaneous tumors were detected by IHC staining, scale bar = 50 μm. siNC, negative control; siDDX11-AS1, DDX11-AS1 knockdown. *$p < 0.05$.

staining revealed a significant reduction in the expression of two cell proliferation indicators (Ki67 and PCNA) in the xenograft tumor tissues following the knockdown of DDX11-AS1, as shown in Figure 4D. Collectively, above results indicate that DDX11-AS1 knockdown can attenuate tumor growth in vivo.

Identification of DDX11-AS1-Controlled Genes in HCC Cells Through RNA-Seq Analysis

To resolve the genes controlled by DDX11-AS1 in HCC cells, RNA-seq was used to probe into transcriptome changes in Bel-7402 cells following DDX11-AS1 knockdown. Under the criteria of |log2 (FC)| being equal to or greater than 0.6 and FDR less than 0.05, a total of 365 differentially expressed genes (DEGs) were pinpointed, involving 211 genes with increased expression and 154 genes with decreased expression (Figure 5A and Supplementary Table S3). Notably, we found that the expression levels of some recognized genes linked to HCC altered following the knockdown of DDX11-AS1, including CTH,[24] GADD45B,[25] PCK2,[26] PHLDA1,[27] TXNIP,[28] AKR1C3,[29] CA9,[16] LRPPRC,[30] MSI2,[31] MTOR,[32] NDUFA4L2,[33] and SMYD3[34] (Figure 5B). To understand the potential roles and signaling pathways influenced by DDX11-AS1 in HCC cells, the DAVID online tool was utilized to conduct the enrichment analysis of GO and KEGG based on DEGs to identify the biological processes and signaling pathways involved in DEGs (Supplementary Table S4 and Supplementary Table S5). As illustrated by Figure 5C, DEGs were significantly enriched

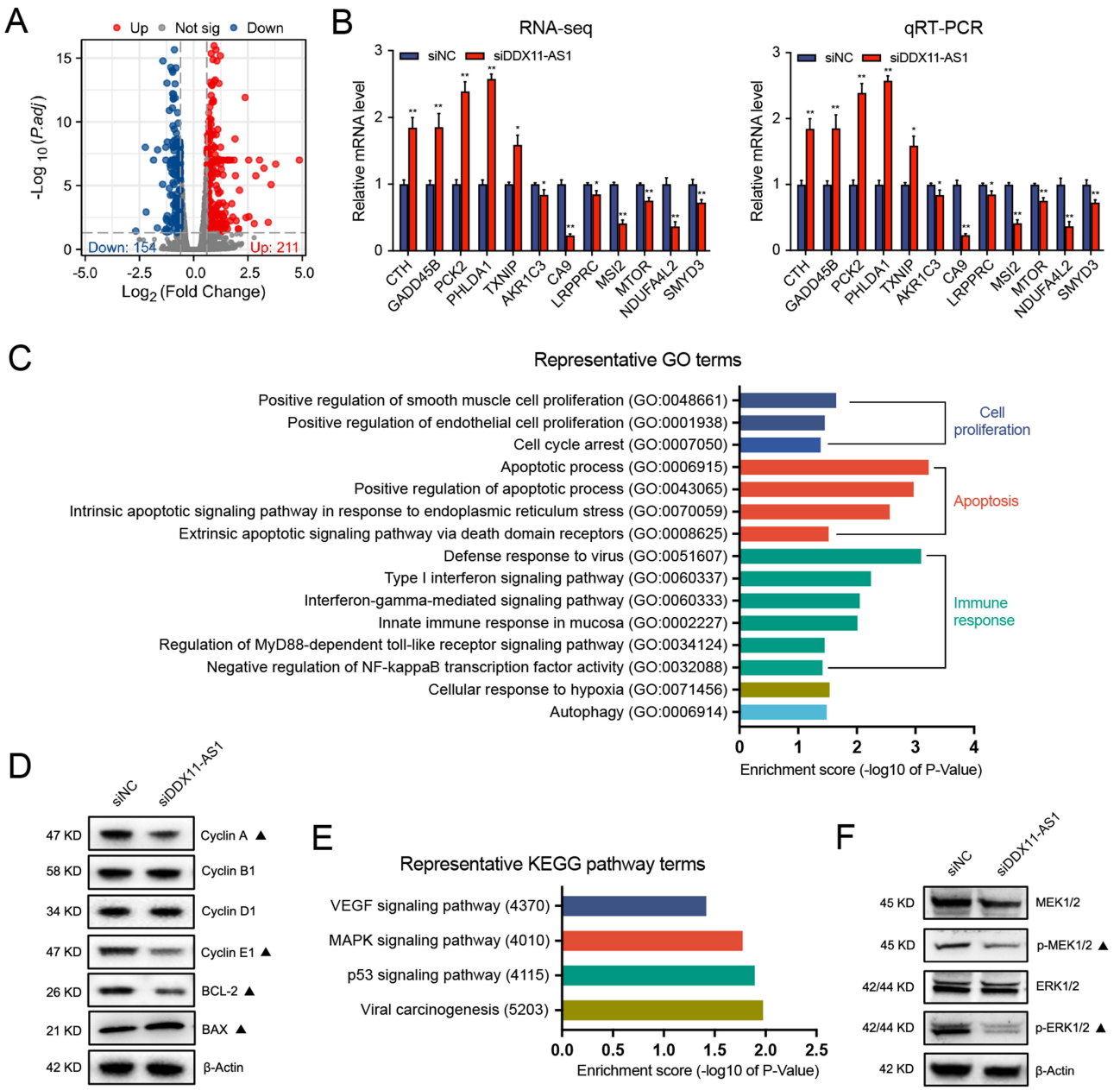

Figure 5 The effect of DDX11-AS1 knockdown on the transcriptome of HCC cells is revealed by RNA-Seq. (**A**) Volcano plots displaying 365 differentially expressed genes (DEGs) between DDX11-AS1 knockdown and negative control Bel-7402 cells with |log2(FC)| ≥ 0.6 and FDR < 0.05. The red and blue points represent genes that were upregulated and downregulated after DDX11-AS1 knockdown, respectively. (**B**) Validation of RNA-Seq results (left) through detecting twelve of known HCC-related genes by qRT-PCR (right). (**C**) Representative GO terms for biological processes (BP) enriched by DEGs. (**D**) The impact of DDX11-AS1 knockdown on the expression of some critical regulators that control cell cycle and apoptosis was examined by Western blotting. (**E**) Representative KEGG pathway terms that enriched by DEGs. (**F**) The impact of DDX11-AS1 knockdown on the activity of MEK/ERK pathway was examined by Western blotting. siNC, negative control; siDDX11-AS1, DDX11-AS1 knockdown. The black triangles (▲) represent genes whose expression changed when DDX11-AS1 was knocked down. *p < 0.05, **p < 0.01.

in cell proliferation, apoptosis, and immune response. In combination with the cell phenotype, we additionally explored the influence of DDX11-AS1 muting on the expression trends of several key regulators involved in the cell cycle and apoptosis process through Western blot, the findings exhibited that silencing of DDX11-AS1 resulted in markedly reduced levels of Cyclin A, Cyclin E1, and the anti-apoptotic protein BCL-2, while also leading to a significant rise in the pro-apoptotic protein BAX (Figure 5D). Furthermore, significant enrichment of DEGs was observed in crucial cancer-associated pathways, including VEGF, MAPK, and p53 signaling (Figure 5E). The MAPK pathway, particularly its central component, the MEK/ERK signaling cascade, has been extensively studied and is

https://doi.org/10.2147/JHC.S516656

recognized for its crucial involvement in the growth and metastasis of HCC.[20,35] In our research, we disclosed that silencing DDX11-AS1 could significantly reduce the phosphorylated MEK1/2 and ERK1/2 levels (Figure 5F), suggesting that DDX11-AS1 might facilitate the HCC advancement through the activation of the MEK/ERK signaling route.

Carbonic Anhydrase IX (CA9), a Downstream Gene of DDX11-AS1, Mediates the Carcinogenic Role of DDX11-AS1 in HCC Cells

As exhibited in Figure 5B, above RNA-seq and qRT-PCR verification data indicated that CA9 expression showed the most substantial change after DDX11-AS1 knockdown. Further analysis of the TCGA data revealed a strong positive link between the expression levels of DDX11-AS1 and CA9 in HCC (Figure 6A), suggesting that CA9 could be a downstream target of DDX11-AS1. Then, the modulatory effect of DDX11-AS1 on CA9 expression was assessed through both qRT-PCR and Western blot analysis, and the findings uncovered that DDX11-AS1 silencing resulted in a substantial decrease in both mRNA and protein levels of CA9 in HCC (Figure 6B and C). Multiple rescue tests were carried out to clarify whether CA9 influenced the impact of DDX11-AS1 on the biological behaviors of HCC cells. The CCK-8 results exhibited that overexpressing CA9 could counteract the prohibitive effect of DDX11-AS1 silencing on cell propagation (Figure 6D). Colony formation assays uncovered that upregulation of CA9 could mitigate the reduction in colony formation potential caused by DDX11-AS1 silencing (Figure 6E). Transwell assays disclosed that the suppressive impact of DDX11-AS1 silencing on cell migration and invasion could be alleviated by increasing CA9 levels (Figure 6F and G). In general, above findings indicate that CA9, acting as a downstream target, plays a mediating role in the carcinogenic effects of DDX11-AS1 in HCC.

DDX11-AS1 Is Activated by the Transcription Factor Nuclear Respiratory Factor 1 (NRF1) in HCC Cells

Numerous researches have uncovered that transcription factors play vital functions in modulating the aberrant expression of lncRNAs in various types of cancer.[36,37] To illustrate the mechanism by which transcription factors modulate the upregulation of DDX11-AS1 in HCC, we initially inquired the transcription factor binding sites within the DDX11-AS1 promoter region using transcription factor ChIP-seq track of the UCSC Genome Browser Gateway (https://genome.ucsc.edu/cgi-bin/hgGateway). As illustrated in Figure 7A, the promoter area of DDX11-AS1 exhibits strong ChIP-seq signals for several well-known oncogenic transcription factors, such as NRF1,[38] ZEB2,[39] and c-MYC.[40] It is noteworthy that NRF1 exhibits the strongest binding signal and is also present in HepG2 cells, indicating that NRF1 potentially has a vital role in managing the expression of DDX11-AS1 in HCC cells. Subsequently, we utilized TCGA data to investigate the expression link between DDX11-AS1 and NRF1 in HCC, and we identified a substantial positive association between the expression levels of DDX11-AS1 and NRF1 in HCC (Figure 7B). We further clarified the regulatory role of NRF1 on DDX11-AS1 by qRT-PCR. As indicated by Figure 7C and D, the expression levels of NRF1 were effectively downregulated and upregulated in HCC cells, and silencing NRF1 led to a reduction in DDX11-AS1 expression, whereas overexpressing NRF1 resulted in an elevated expression of DDX11-AS1 in HCC cells. To find out whether NRF1 controls DDX11-AS1 expression at the transcriptional level, we used dual-luciferase reporter assays to detect the modulatory impact of NRF1 on the promoter activity of DDX11-AS1 in HCC cells, and the findings displayed that reducing NRF1 expression led to diminished promoter activity, while increasing NRF1 expression boosted the promoter activity of DDX11-AS1 (Figure 7E). The NRF1 binding site within the promoter area of DDX11-AS1 was predicted using the JASPAR online tool (https://jaspar.elixir.no/), and a highly potential NRF1 binding motif, located between −325 to −257 bp (ACGCTGGCCCG; relative profile score > 0.85), was identified. According to the ChIP-qPCR results, DNA fragments containing NRF1-binding motifs were notably enriched, whereas those lacking these motifs were not (Figure 7F and G), hinting that NRF1 is capable of directly binding to the promoter of DDX11-AS1. Together, these findings indicate that DDX11-AS1 can be positively controlled by NRF1 in HCC cells.

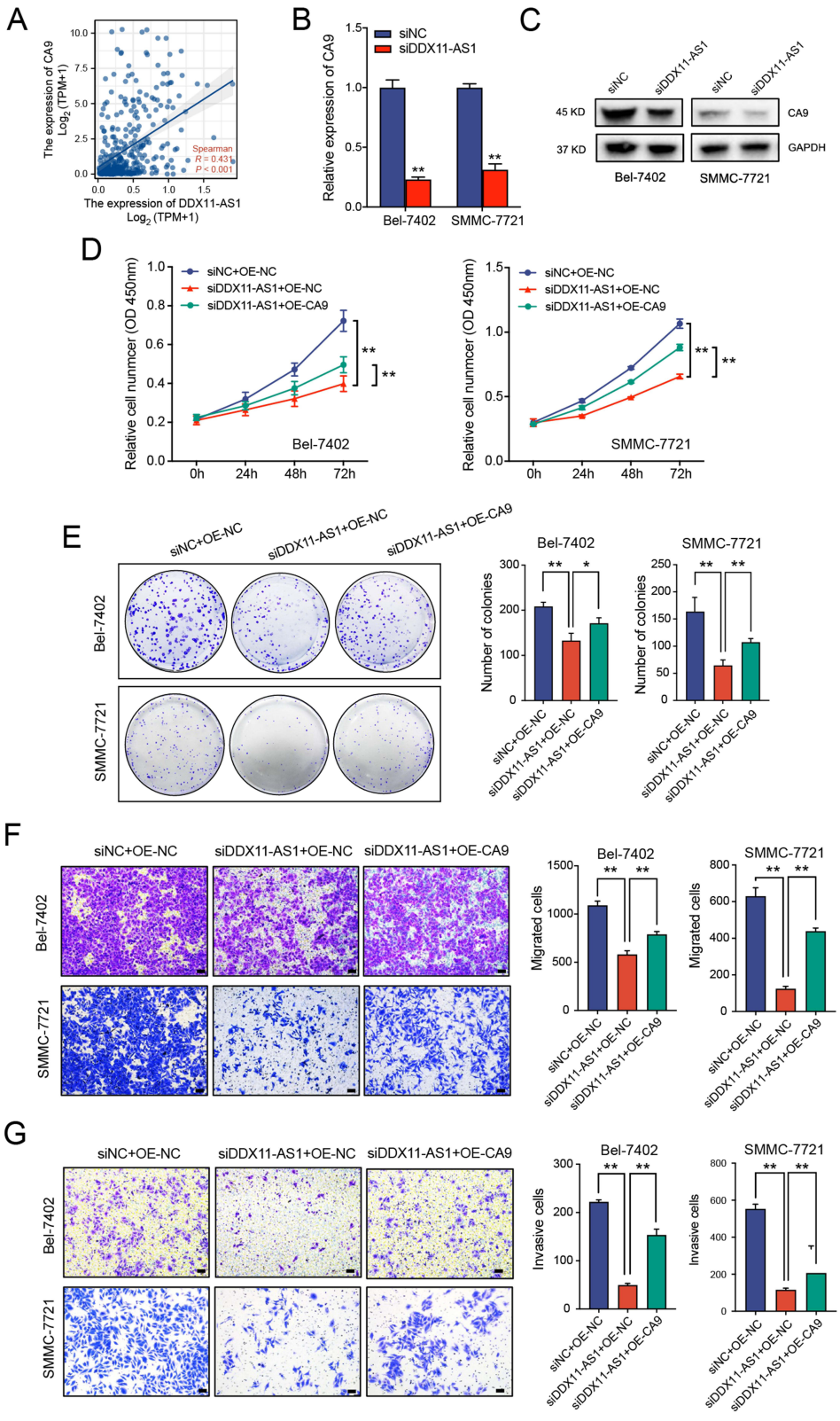

Figure 6 CA9-mediated the oncogenic phenotypes of DDX11-AS1 in HCC cells was confirmed by rescue experiments. (**A**) Correlation analysis between the expression of DDX11-AS1 and CA9 in HCC based on TCGA data. The regulatory effect of DDX11-AS1 on CA9 was validated by qRT-PCR (**B**) and Western blotting (**C**). Overexpression of CA9 attenuates the suppressive effects of DDX11-AS1 knockdown on the capacities of cell proliferation (**D**), colony formation (**E**), migration (**F**), and invasion (**G**). siNC, negative control; siDDX11-AS1, DDX11-AS1 knockdown; OE-NC, empty overexpression vector; OE-CA9, CA9 overexpression. Scale bar = 100 μm. *$p < 0.05$, **$p < 0.01$.

https://doi.org/10.2147/JHC.S516656

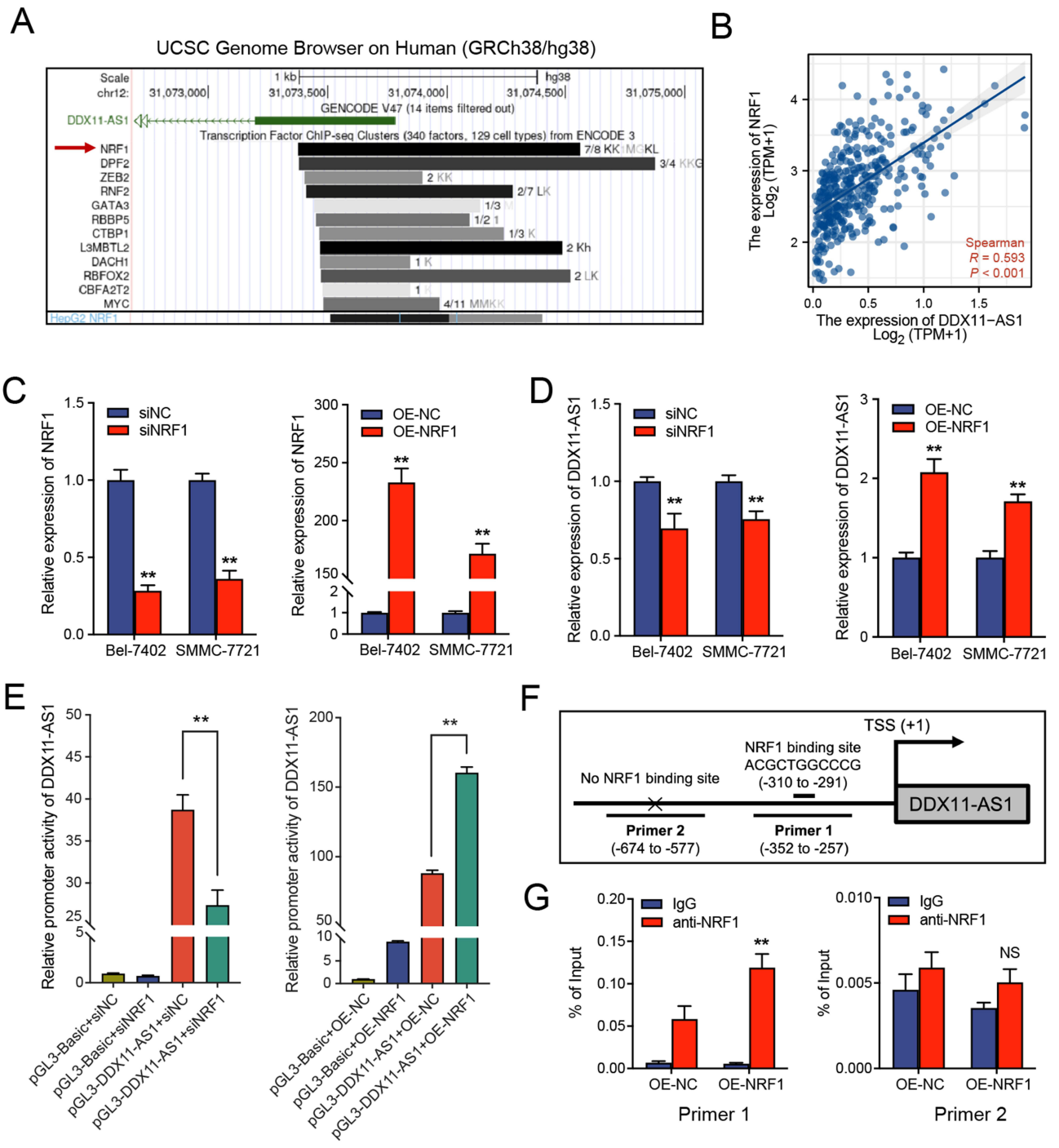

Figure 7 DDX11-AS1 can be positively regulated by the transcription factor NRF1 in HCC cells. (**A**) The ChIP-seq data from the UCSC Genome Browser indicates a strong ChIP-seq signal of NRF1 within the promoter region of DDX11-AS1 (red arrow). (**B**) Correlation analysis between the expression of DDX11-AS1 and NRF1 in HCC based on TCGA data. (**C**) The knockdown and overexpression efficiency of NRF1 in HCC cells was determined by qRT-PCR. (**D**) The effect of knockdown or overexpression of NRF1 on DDX11-AS1 expression was validated by qRT-PCR. (**E**) The effect of knockdown or overexpression of NRF1 on the promoter activity of DDX11-AS1 was evaluated by dual-luciferase reporter assay. (**F**) Schematic diagram of NRF1 binding site within DDX11-AS1 promoter region and amplification position of ChIP-qPCR primers. (**G**) The binding abundance of NRF1 on the DDX11-AS1 promoter upon NRF1 overexpression was detected by ChIP-qPCR. siNC, negative control; siDDX11-AS1, DDX11-AS1 knockdown; OE-NC, empty vector; OE-NRF1, NRF1 overexpression; pGL3-Basic, pGL3-Basic empty vector; pGL3-DDX11-AS1, pGL3-Basic vector inserting the DDX11-AS1 promoter. TSS, transcription start site. $^{**}p < 0.01$.

Discussion

DDX11-AS1, a cell cycle-associated lncRNA, has been identified as a cancer-promoting molecule that contributes to the advancement of multiple cancers, including HCC. In the current research, we thoroughly examined the clinical importance of DDX11-AS1 in HCC, as well as its functional role and mechanisms in HCC progression.

First, the expression pattern and clinical relevance of DDX11-AS1 in HCC were probed through comprehensive bioinformatics study. We unveiled that high DDX11-AS1 expression correlates with adverse clinicopathological characteristics (T stage, histologic grade, vascular invasion, and AFP level) and unfavorable prognosis (OS, DSS, PFI) in HCC patients. Furthermore, DDX11-AS1 was identified as an independent factor that prognostically affecting OS, exhibiting significant predictive and diagnostic potential for HCC and patient survival outcomes. Consistent with our findings, increased DDX11-AS1 expression is positively linked to WHO grade, OS, and disease-free survival (DFS) in glioma (GM) patients, and it shows great precision in forecasting the prognosis.[41] As for HCC, interestingly, recent studies have found that cuproptosis and ferroptosis-related lncRNA signatures, composed of DDX11-AS1 and other lncRNAs, can serve as effective predictors of prognosis and immune response in HCC patients.[42,43] Notably, a 2022 study revealed that DDX11-AS1 is a useful marker for discriminating HCC tissues from normal nontumor specimens through detecting the expression of DDX11-AS1 in human HCC tissues and conducting the ROC analysis,[44] suggesting the potential of DDX11-AS1 used as a diagnostic biomarker for HCC patients. If DDX11-AS1 can be detected in the serum or exosomes of peripheral blood and its expression level has a good diagnostic effect, the clinical translational value of DDX11-AS1 as a diagnostic marker for HCC would be greatly enhanced.

Secondly, the subcellular localization study indicated that DDX11-AS1 is chiefly situated in the nucleus of HCC cells, although it is also present in the cytoplasm, implying that DDX11-AS1 potentially affects HCC by regulating transcriptional or post-transcriptional processes. Consistent with these findings in HCC cells, DDX11-AS1 was also predominantly situated in the nucleus in lung cancer cells A549 as well as colon cancer cells HCT116.[7] However, in esophageal squamous cell carcinoma (ESCC) cells, it is interesting to note that DDX11-AS1 was reported to be primarily located in the cytoplasm instead of the nucleus,[45] indicating that the subcellular distribution of DDX11-AS1 varies across different types of tumor cells, which may reflect distinct molecular mechanisms underlying its function in different cancers.

Third, loss-of-function assays unveiled that muting DDX11-AS1 could impede the activity of propagation, migration, and invasion of HCC cells, hinting that DDX11-AS1 acts as a cancer promoter in HCC. Likewise, researches on BC and ESCC demonstrated that DDX11-AS1 serves as an oncogene, promoting tumor development by facilitating cell proliferation, migration, and invasion.[8,45] Moreover, our findings uncovered that reducing DDX11-AS1 levels could stop the cell cycle of HCC cells at the S and G2/M stages, implying that DDX11-AS1 could control HCC cell growth by managing the cell cycle. Interestingly, in A549 lung cancer cells, DDX11-AS1 was disclosed to impede cell growth by inducing a G0/G1 cell cycle halt, suggesting that DDX11-AS1 is capable of modulating the cell cycle process through different mechanisms in various cancer cells. Furthermore, we observed that silencing DDX11-AS1 can boost the apoptosis of HCC cells, suggesting that DDX11-AS1 facilitates HCC growth by inhibiting apoptosis. Recent research suggests that DDX11-AS1 can enhance sorafenib resistance of HCC cells through suppressing ferroptosis,[13] indicating that DDX11-AS1 is involved in controlling the multiple programmed cell death (PCD) pathway.

Fourth, the possible DDX11-AS1-modulated genes in HCC cells were identified through RNA-seq analysis, and 365 DEGs were found to exhibit abnormal expression following DDX11-AS1 silencing in Bel-7402 cells. GO analysis disclosed DEGs could be enriched in terms associated with immune response, in addition to those concerning cell proliferation and apoptosis, suggesting that DDX11-AS1 might contribute to its oncogenic activity by influencing the immune response. A bioinformatics analysis revealed that a ferroptosis-related nine-lncRNA signature which includes DDX11-AS1 is closely associated with immune cell infiltration in HCC.[43] KEGG analysis identified DEGs linked to the MAPK, VEGF, and p53 signaling pathways. In this study, the impact of DDX11-AS1 on the MAPK pathway in HCC cells was verified by observing alterations in the MEK/ERK cascade, a crucial segment of the MAPK signaling. To date, numerous lncRNAs have been demonstrated to accelerate HCC development through the activation of the MEK/ERK signaling route, especially some homeobox (HOX) cluster-embedded lncRNAs, such as HOXD-AS1,[21] HOXD-AS2,[22] HOXA-A3.[46] Interestingly, in ESCC, DDX11-AS1 was revealed to positively regulate the Wnt/β-catenin signaling,[45] while in non-small cell lung cancer (NSCLC), it was shown to activate PI3K/AKT signaling,[47] indicating that the signaling pathways influenced by DDX11-AS1 may differ across various types of tumors.

Fifth, previous studies have disclosed some downstream genes of DDX11-AS1 in HCC, such as p53,[12] MACC1,[48] and LATS2.[49] In the current research, CA9 was identified as a novel downstream gene of DDX11-AS1, and its expression level is positively regulated by DDX11-AS1, which can mediate the promotional influence of DDX11-AS1 on HCC progression. CA9, a transmembrane dimeric metalloenzyme, belongs to the alpha-carbonic anhydrase family which responsible for the reversible hydration of carbon dioxide to bicarbonate ions and protons to maintain intracellular pH homeostasis.[50] As a well-characterized

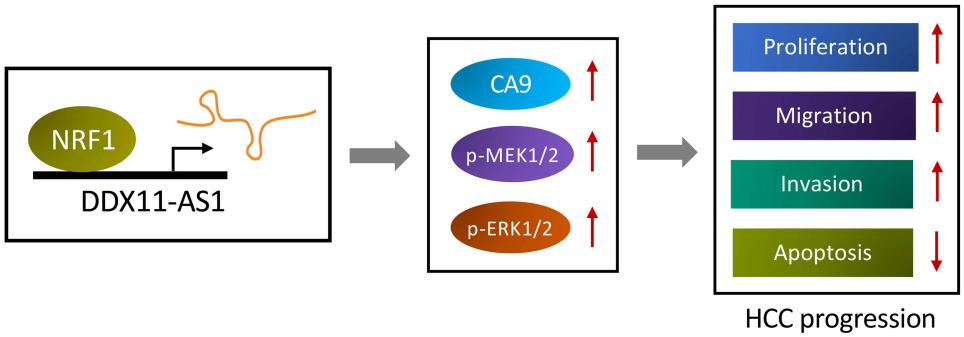

Figure 8 Schematic diagram of the mechanism by which NRF1-regulated DDX11-AS1 facilitates HCC progression.

oncogene, CA9 contributes extensively to the pathogenesis and progression of various malignancies.[15] For HCC, it has been revealed that CA9 can be upregulated under hypoxic conditions and play a critical function in HCC development through affecting cell propagation, apoptosis, and EMT.[16,18] Recent studies found that CA9 can be regulated by other lncRNAs and mediate tumor progression, such as LINC02086 in pancreatic cancer (PC) and ZNF674-AS1 in neuroblastoma (NB).[51,52] Noteworthily, the current study is the first to identify a lncRNA that can regulate CA9 expression in HCC.

Ultimately, we found that the transcription factor NRF1 can enhance the expression level of DDX11-AS1 by directly targeting its promoter in HCC cells, thus revealing the mechanism responsible for the aberrant expression of DDX11-AS1 in HCC. NRF1, a transcription factor that manages nuclear genes needed for respiration, heme biosynthesis, and mitochondrial DNA transcription and replication,[53] has been found to be critically involved in tumor development by functioning as a cancer-promoting transcription factor. In HCC, for example, NRF1 has been identified as an oncogene that can promote the progression of HCC by targeting LPCAT1 and E2F1.[38,54] Here, we reveal that DDX11-AS1 is a novel target gene of NRF1.

In this study, DDX11-AS1 was found to be a potential diagnostic marker and therapeutic target for HCC as an oncogenic lncRNA. Subsequently, the expression of DDX11-AS1 in the peripheral blood serum or exosomes of HCC patients and its diagnostic value for HCC should be further clarified, and the therapeutic effect of siRNAs specifically targeting DDX11-AS1 in HCC should be evaluated by animal experiments, thereby significantly enhancing the possibility of clinical application of DDX11-AS1.

Conclusion

In summary, this paper disclosed that NRF1 transcriptionally activates lncRNA DDX11-AS1 to facilitate HCC progression via elevating CA9 expression and activating the MEK/ERK signaling cascade (Figure 8), implying that DDX11-AS1 holds promise as a potential diagnostic and prognostic biomarker and therapeutic target for HCC.

Data Sharing Statement

The data that support the findings of this study are available from the corresponding author upon reasonable request.

Ethics Statement

The study was approved by the Ethics Committee of Xi'an Jiaotong University Health Science Center (No. 2020-738).

Acknowledgments

We would like to thank the other members of our research team for their assistance. We are also grateful to the TCGA database for providing access to the public data.

Funding

This research was funded by the Natural Science Foundation Research Program of Shaanxi Province of China (2023-JC-YB-750 and 2023-JC-YB-700), and the Science Research Foundation of the Second Affiliated Hospital of Xi'an Jiaotong University (YJ(ZYTS)2019046).

Disclosure

The authors declare no conflicts of interest.

References

1. Koshy A. Evolving global etiology of hepatocellular Carcinoma (HCC): insights and trends for 2024. *J Clin Exp Hepatol*. 2025;15(1):102406. doi:10.1016/j.jceh.2024.102406
2. Singal AG, Kanwal F, Llovet JM. Global trends in hepatocellular carcinoma epidemiology: implications for screening, prevention and therapy. *Nat Rev Clin Oncol*. 2023;20(12):864–884. doi:10.1038/s41571-023-00825-3
3. Yang H, Liu Y, Zhang N, Tao F, Yin G. Therapeutic advances in hepatocellular carcinoma: an update from the 2024 ASCO annual meeting. *Front Oncol*. 2024;14:1453412. doi:10.3389/fonc.2024.1453412
4. Mattick JS, Amaral PP, Carninci P, et al. Long non-coding RNAs: definitions, functions, challenges and recommendations. *Nat Rev Mol Cell Biol*. 2023;24(6):430–447. doi:10.1038/s41580-022-00566-8
5. Naseer QA, Malik A, Zhang F, Chen S. Exploring the enigma: history, present, and future of long non-coding RNAs in cancer. *Discov Oncol*. 2024;15(1):214. doi:10.1007/s12672-024-01077-y
6. Liang W, Zhao Y, Meng Q, Jiang W, Deng S, Xue J. The role of long non-coding RNA in hepatocellular carcinoma. *Aging*. 2024;16(4):4052–4073. doi:10.18632/aging.205523
7. Marchese FP, Grossi E, Marin-Bejar O, et al. A long noncoding RNA regulates sister chromatid cohesion. *Mol Cell*. 2016;63(3):397–407. doi:10.1016/j.molcel.2016.06.031
8. Li Y, Zhou M, Yang L, et al. LncRNA DDX11-AS1 promotes breast cancer progression by targeting the miR-30c-5p/MTDH axis. *Sci Rep*. 2024;14(1):26745. doi:10.1038/s41598-024-78413-3
9. Si X, Zhang G, Li M, et al. LncRNA DDX11-AS1 promotes chemoresistance through LIN28A-mediated ATG12 mRNA stabilization in breast cancer. *Pharmacology*. 2023;108(1):61–73. doi:10.1159/000527222
10. Wu C, Wang Z, Tian X, Wang J, Zhang Y, Wu B. Long non-coding RNA DDX11-AS1 promotes esophageal carcinoma cell proliferation and migration through regulating the miR-514b-3p/RBX1 axis. *Bioengineered*. 2021;12(1):3772–3786. doi:10.1080/21655979.2021.1940617
11. Zhang S, Jiang H, Xu Z, et al. The resistance of esophageal cancer cells to paclitaxel can be reduced by the knockdown of long noncoding RNA DDX11-AS1 through TAF1/TOP2A inhibition. *Am J Cancer Res*. 2019;9(10):2233–2248.
12. Xu M, Zhao X, Zhao S, et al. Landscape analysis of lncRNAs shows that DDX11-AS1 promotes cell-cycle progression in liver cancer through the PARP1/p53 axis. *Cancer Lett*. 2021;520:282–294. doi:10.1016/j.canlet.2021.08.001
13. Wang L, Wang L. Long noncoding RNA DDX11-AS1 represses sorafenib-induced ferroptosis in hepatocellular carcinoma cells via Nrf2-Keap1 pathway. *Discov Oncol*. 2024;15(1):544. doi:10.1007/s12672-024-01431-0
14. Ding G, Zeng Y, Yang D, et al. Correction to: silenced lncRNA DDX11-AS1 or up-regulated microRNA-34a-3p inhibits malignant phenotypes of hepatocellular carcinoma cells via suppression of TRAF5. *Cancer Cell Int*. 2021;21(1):659. doi:10.1186/s12935-021-02360-6
15. Pastorekova S, Gillies RJ. The role of carbonic anhydrase IX in cancer development: links to hypoxia, acidosis, and beyond. *Cancer Metastasis Rev*. 2019;38(1–2):65–77. doi:10.1007/s10555-019-09799-0
16. Yu SJ, Yoon JH, Lee JH, et al. Inhibition of hypoxia-inducible carbonic anhydrase-IX enhances hexokinase II inhibitor-induced hepatocellular carcinoma cell apoptosis. *Acta Pharmacol Sin*. 2011;32(7):912–920. doi:10.1038/aps.2011.24
17. Cho EJ, Yu SJ, Kim K, et al. Carbonic anhydrase-IX inhibition enhances the efficacy of hexokinase II inhibitor for hepatocellular carcinoma in a murine model. *J Bioenerg Biomembr*. 2019;51(2):121–129. doi:10.1007/s10863-019-09788-6
18. Hyuga S, Wada H, Eguchi H, et al. Expression of carbonic anhydrase IX is associated with poor prognosis through regulation of the epithelial-mesenchymal transition in hepatocellular carcinoma. *Int J Oncol*. 2017;51(4):1179–1190. doi:10.3892/ijo.2017.4098
19. Zheng J, Wang S, Xia L, et al. Hepatocellular carcinoma: signaling pathways and therapeutic advances. *Signal Transduct Target Ther*. 2025;10(1):35. doi:10.1038/s41392-024-02075-w
20. Moon H, Ro SW. MAPK/ERK signaling pathway in hepatocellular carcinoma. *Cancers*. 2021;13(12):3026. doi:10.3390/cancers13123026
21. Sun J, Guo Y, Bie B, et al. Silencing of long noncoding RNA HOXD-AS1 inhibits proliferation, cell cycle progression, migration and invasion of hepatocellular carcinoma cells through MEK/ERK pathway. *J Cell Biochem*. 2020;121(1):443–457. doi:10.1002/jcb.29206
22. Sun J, Li Y, Shi M, et al. A positive feedback loop of lncRNA HOXD-AS2 and SMYD3 facilitates hepatocellular carcinoma progression via the MEK/ERK pathway. *J Hepatocell Carcinoma*. 2023;10:1237–1256. doi:10.2147/JHC.S416946
23. Mas-Ponte D, Carlevaro-Fita J, Palumbo E, Hermoso Pulido T, Guigo R, Johnson R. LncATLAS database for subcellular localization of long noncoding RNAs. *RNA*. 2017;23(7):1080–1087. doi:10.1261/rna.060814.117
24. Lin Z, Huang W, He Q, et al. FOXC1 promotes HCC proliferation and metastasis by Upregulating DNMT3B to induce DNA Hypermethylation of CTH promoter. *J Exp Clin Cancer Res*. 2021;40(1):50. doi:10.1186/s13046-021-01829-6
25. Ma D, Shen B, Seewoo V, et al. GADD45beta induction by S-adenosylmethionine inhibits hepatocellular carcinoma cell proliferation during acute ischemia-hypoxia. *Oncotarget*. 2016;7(24):37215–37225. doi:10.18632/oncotarget.9295
26. Liu MX, Jin L, Sun SJ, et al. Metabolic reprogramming by PCK1 promotes TCA cataplerosis, oxidative stress and apoptosis in liver cancer cells and suppresses hepatocellular carcinoma. *Oncogene*. 2018;37(12):1637–1653. doi:10.1038/s41388-017-0070-6
27. Yao B, Niu Y, Li Y, Chen T, Wei X, Liu Q. High-matrix-stiffness induces promotion of hepatocellular carcinoma proliferation and suppression of apoptosis via miR-3682-3p-PHLDA1-FAS pathway. *J Cancer*. 2020;11(21):6188–6203. doi:10.7150/jca.45998
28. Sheth SS, Bodnar JS, Ghazalpour A, et al. Hepatocellular carcinoma in Txnip-deficient mice. *Oncogene*. 2006;25(25):3528–3536. doi:10.1038/sj.onc.1209394
29. Wu C, Dai C, Li X, et al. AKR1C3-dependent lipid droplet formation confers hepatocellular carcinoma cell adaptability to targeted therapy. *Theranostics*. 2022;12(18):7681–7698. doi:10.7150/thno.74974
30. Wang H, Tang A, Cui Y, Gong H, Li H. LRPPRC facilitates tumor progression and immune evasion through upregulation of m(6)A modification of PD-L1 mRNA in hepatocellular carcinoma. *Front Immunol*. 2023;14:1144774. doi:10.3389/fimmu.2023.1144774

31. Wang MH, Qin SY, Zhang SG, et al. Musashi-2 promotes hepatitis Bvirus related hepatocellular carcinoma progression via the Wnt/beta-catenin pathway. *Am J Cancer Res*. 2015;5(3):1089–1100.
32. Ferrin G, Guerrero M, Amado V, Rodriguez-Peralvarez M, De la Mata M. Activation of mTOR signaling pathway in hepatocellular carcinoma. *Int J Mol Sci*. 2020;21(4):1266. doi:10.3390/ijms21041266
33. Lai RK, Xu IM, Chiu DK, et al. NDUFA4L2 fine-tunes oxidative stress in hepatocellular carcinoma. *Clin Cancer Res*. 2016;22(12):3105–3117. doi:10.1158/1078-0432.CCR-15-1987
34. Ding Q, Cai J, Jin L, et al. A novel small molecule ZYZ384 targeting SMYD3 for hepatocellular carcinoma via reducing H3K4 trimethylation of the Rac1 promoter. *MedComm*. 2024;5(10):e711. doi:10.1002/mco2.711
35. Xue Y, Ruan Y, Wang Y, Xiao P, Xu J. Signaling pathways in liver cancer: pathogenesis and targeted therapy. *Mol Biomed*. 2024;5(1):20. doi:10.1186/s43556-024-00184-0
36. Li D, Yang W, Zhang J, Yang JY, Guan R, Yang MQ. Transcription factor and lncRNA regulatory networks identify key elements in lung adenocarcinoma. *Genes*. 2018;9(1):12. doi:10.3390/genes9010012
37. Jasim SA, Almajidi YQ, Al-Rashidi RR, et al. The interaction between lncRNAs and transcription factors regulating autophagy in human cancers: a comprehensive and therapeutical survey. *Cell Biochem Funct*. 2024;42(2):e3971. doi:10.1002/cbf.3971
38. Liu R, Yin C, Zhao P, et al. Nuclear respiratory factor 1 drives hepatocellular carcinoma progression by activating LPCAT1-ERK1/2-CREB axis. *Biol Direct*. 2023;18(1):67. doi:10.1186/s13062-023-00428-z
39. Xia L, Huang W, Tian D, et al. Forkhead box Q1 promotes hepatocellular carcinoma metastasis by transactivating ZEB2 and VersicanV1 expression. *Hepatology*. 2014;59(3):958–973. doi:10.1002/hep.26735
40. Liu F, Liao Z, Zhang Z. MYC in liver cancer: mechanisms and targeted therapy opportunities. *Oncogene*. 2023;42(45):3303–3318. doi:10.1038/s41388-023-02861-w
41. Xiang Z, Lv Q, Zhang Y, et al. Long non-coding RNA DDX11-AS1 promotes the proliferation and migration of glioma cells by combining with HNRNPC. *Mol Ther Nucleic Acids*. 2022;28:601–612. doi:10.1016/j.omtn.2022.04.016
42. Li Y, Song K, Zheng W. The cuproptosis-related long noncoding RNA signature predicts prognosis and immune cell infiltration in hepatocellular carcinoma. *J Oncol*. 2023;2023:9557690. doi:10.1155/2023/9557690
43. Xu Z, Peng B, Liang Q, et al. Construction of a ferroptosis-related nine-lncRNA signature for predicting prognosis and immune response in hepatocellular carcinoma. *Front Immunol*. 2021;12:719175. doi:10.3389/fimmu.2021.719175
44. Luo X, Wang Y, Zhang X, Liu W. The clinical value of long noncoding RNA DDX11-AS1 as a biomarker for the diagnosis and prognosis of hepatocellular carcinoma. *J Oncol*. 2022;2022:5735462. doi:10.1155/2022/5735462
45. Guo Y, Sun P, Guo W, et al. LncRNA DDX11 antisense RNA 1 promotes EMT process of esophageal squamous cell carcinoma by sponging miR-30d-5p to regulate SNAI1/ZEB2 expression and Wnt/beta-catenin pathway. *Bioengineered*. 2021;12(2):11425–11440. doi:10.1080/21655979.2021.2008759
46. Tong Y, Wang M, Dai Y, Bao D, Zhang J, Pan H. LncRNA HOXA-AS3 sponges miR-29c to facilitate cell proliferation, metastasis, and EMT process and activate the MEK/ERK signaling pathway in hepatocellular carcinoma. *Hum Gene Ther Clin Dev*. 2019;30(3):129–141. doi:10.1089/humc.2018.266
47. Feng X, Yang S, Zhou S, Deng S, Xie Y. Long non-coding RNA DDX11-AS1 promotes non-small cell lung cancer development via regulating PI3K/AKT signalling. *Clin Exp Pharmacol Physiol*. 2020;47(9):1622–1631. doi:10.1111/1440-1681.13325
48. Wan T, Zheng J, Yao R, Yang S, Zheng W, Zhou P. LncRNA DDX11-AS1 accelerates hepatocellular carcinoma progression via the miR-195-5p/MACC1 pathway. *Ann Hepatol*. 2021;20:100258. doi:10.1016/j.aohep.2020.09.003
49. Li Y, Zhuang W, Huang M, Li X. Long noncoding RNA DDX11-AS1 epigenetically represses LATS2 by interacting with EZH2 and DNMT1 in hepatocellular carcinoma. *Biochem Biophys Res Commun*. 2019;514(4):1051–1057. doi:10.1016/j.bbrc.2019.05.042
50. Ronca R, Supuran CT. Carbonic anhydrase IX: an atypical target for innovative therapies in cancer. *Biochim Biophys Acta Rev Cancer*. 2024;1879(4):189120. doi:10.1016/j.bbcan.2024.189120
51. Xiong Y, Kong X, Tu S, et al. LINC02086 inhibits ferroptosis and promotes malignant phenotypes of pancreatic cancer via miR-342-3p/CA9 axis. *Funct Integr Genomics*. 2024;24(2):49. doi:10.1007/s10142-024-01329-8
52. Zhao K, Wang X, Jin Y, et al. LncRNA ZNF674-AS1 drives cell growth and inhibits cisplatin-induced pyroptosis via up-regulating CA9 in neuroblastoma. *Cell Death Dis*. 2024;15(1):5. doi:10.1038/s41419-023-06394-8
53. Scarpulla RC. Transcriptional paradigms in mammalian mitochondrial biogenesis and function. *Physiol Rev*. 2008;88(2):611–638. doi:10.1152/physrev.00025.2007
54. Wang D, Wan B, Zhang X, et al. Nuclear respiratory factor 1 promotes the growth of liver hepatocellular carcinoma cells via E2F1 transcriptional activation. *BMC Gastroenterol*. 2022;22(1):198. doi:10.1186/s12876-022-02260-7

Journal of Hepatocellular Carcinoma

Dovepress
Taylor & Francis Group

Publish your work in this journal

The Journal of Hepatocellular Carcinoma is an international, peer-reviewed, open access journal that offers a platform for the dissemination and study of clinical, translational and basic research findings in this rapidly developing field. Development in areas including, but not limited to, epidemiology, vaccination, hepatitis therapy, pathology and molecular tumor classification and prognostication are all considered for publication. The manuscript management system is completely online and includes a very quick and fair peer-review system, which is all easy to use. Visit http://www.dovepress.com/testimonials.php to read real quotes from published authors.

Submit your manuscript here: https://www.dovepress.com/journal-of-hepatocellular-carcinoma-journal